THE JOURNAL OF BIOLOGICAL CHEMISTRY
Vol. 269, No. 12, Issue of March 25, pp. 8667–8674, 1994
Printed in U.S.A.

Pyridine Nucleotide Redox Potential Modulates Cystic Fibrosis Transmembrane Conductance Regulator Cl^- Conductance*

(Received for publication, March 29, 1993, and in revised form, November 29, 1993)

M. Jackson Stutts‡, Sherif E. Gabriel, Elmer M. Price, Balazs Sarkadi, John C. Olsen, and Richard C. Boucher

From the Cystic Fibrosis Research Center, Lineberger Cancer Center, Departments of Medicine and Pharmacology, University of North Carolina, Chapel Hill, North Carolina 27599-7020

Cl^- conductance of the apical membrane of airway epithelial cells has properties of a passive diffusion mechanism but is decreased by inhibition of oxidative metabolism. Recent reports that cAMP-dependent Cl^- conductance also requires ATP at the intracellular domains of the cystic fibrosis transmembrane conductance regulator (CFTR) suggest that ATP concentration could mediate metabolic regulation of Cl^- conductance. However, metabolic inhibitors affect processes other than ATP free energy levels, including notably the metabolic pathways that set the redox potential of pyridine nucleotides within the cell. We have investigated the possibility that CFTR-mediated Cl^- conductance is affected by the ratio of oxidized to reduced intracellular pyridine nucleotides. CFTR was expressed in airway and heterologous cells and studied under whole cell voltage clamp conditions, which permitted the intracellular $NAD(P)^+$/NAD(P)H ratio to be varied independently of ATP concentration. In three cell types expressing CFTR, whole cell dialysis with reduced pyridine nucleotides inhibited activation of Cl^- currents by forskolin and 8-(4-chlorophenylthio)-cAMP (CPT-cAMP), whereas dialysis with oxidized pyridines increased both basal and stimulated CFTR-mediated Cl^- conductance. In cell-attached membrane patches, the open probability of 5–6-picosiemens Cl^- channels that had been activated by forskolin and CPT-cAMP was further and reversibly increased by permeant oxidants. Neither swelling-induced whole cell K^+ currents in CFTR-expressing cells nor swelling-induced whole cell Cl^- currents in multidrug resistance protein-expressing cells were affected by NADPH. Pyridine nucleotide redox potential had little effect on phosphorylation of histone by protein kinase A. We conclude that CFTR Cl^- conductance function can be modulated by pyridine nucleotide redox potential. This effect points to the existence of a mechanism or mechanisms by which cytosolic nucleotides other than ATP can affect plasma membrane Cl^- conductance and may help explain how a passive ion conductance is linked to cellular energy metabolism.

In a previous study, exposure of dog bronchial epithelium to NaCN or hypoxia inhibited cAMP-dependent Cl^- conductance (1). Although one mechanism of this effect could be decreased protein phosphorylation caused by depletion of intracellular ATP, we reasoned that it was unlikely that hypoxia or NaCN could drive intracellular ATP concentrations below the K_m for ATP of cAMP-dependent protein kinases of ≈3 μM (2). Recently, an integral membrane protein called CFTR[1] has been identified as the Cl^- channel underlying cAMP-activated apical membrane Cl^- conductance of Cl^--secreting epithelia (3). The predicted amino acid sequence of CFTR placed it as a member of the ATP-binding cassette protein superfamily (4). Other ATP-binding cassette proteins, such as multidrug resistance (MDR) protein, bacterial permeases, and sterile-6, are solute transporters that hydrolyze ATP (5). Sequences contained within CFTR are highly homologous to the putative nucleotide binding folds of MDR protein (6) Recently, it was reported that hydrolyzable nucleotides were required to support CFTR Cl^- channel activity in excised membrane patches, and the K_m of ATP for this requirement was 300 μM (7). In contrast, in human sweat ducts, CFTR-mediated Cl^- conductance was supported by ATP and nonhydrolyzable ATP analogs, with an apparent K_m estimated at several mM (8). The results of these studies suggest that changes in the intracellular concentration of ATP could link cAMP-dependent Cl^- conductance to metabolism through a requirement of CFTR for intracellular ATP.

Beyond maintaining ATP levels, however, substrate metabolism affects other intracellular conditions that influence diverse cellular functions. For example, inhibition of oxidative metabolism by NaCN or hypoxia depletes intracellular ATP by preventing the transfer of electrons extracted from metabolic substrates to oxygen. This results in an increase in the intracellular ratio of reduced to oxidized species of electron carriers, including the pyridine nucleotides (9). This change in redox potential is transmitted throughout the cell because of the wide participation of pyridine nucleotides as cosubstrates in enzymatic processes. In particular, redox potential controls protein-protein associations by affecting the formation of disulfide bonds (10). Ran and Benos (11) found that disulfide bond formation promoted by oxidizing conditions led to multichannel activity and greater conductance in reconstitution studies of epithelial anion channels. Modulation of ion channel activity by intracellular redox potential has been reported in a number of cells (12, 13).

The Cl^- conductance function of CFTR has been well characterized in heterologous expression systems, in which nonpolarized cells infected with viral constructs containing recombinant human CFTR cDNA respond to elevation of intracellular cAMP with increased Cl^- conductance (15–18). The character-

* The costs of publication of this article were defrayed in part by the payment of page charges. This article must therefore be hereby marked "*advertisement*" in accordance with 18 U.S.C. Section 1734 solely to indicate this fact.

‡ To whom correspondence should be addressed: CB 7020, University of North Carolina, Chapel Hill, NC 27599-7020. Tel.: 919-966-1077; Fax: 919-966-7524.

[1] The abbreviations used are: CFTR, cystic fibrosis transmembrane conductance regulator; MDR, multidrug resistance; TES, *N*-tris(hydroxymethyl)methyl-2-aminoethanesulfonic acid; CPT-cAMP, 8-(4-chlorophenylthio)-cAMP; DIDS, 4,4′-diisothiocyanatostilbene-2,2′-disulfonic acid; PMS, phenazine methosulfate; TBOH, tert-butyl hydroxide; NaMBS, sodium metabisulfite.

istics of this cAMP-dependent Cl^- conductance match those of single Cl^- channels activated by cAMP in Cl^--secreting epithelia (19, 20). In the present study, we measured cAMP-activated whole cell current in CFTR-expressing cells with cytosolic ATP clamped at 3 mM while varying the concentration of reduced and oxidized pyridine nucleotides. We also measured the open probability of CFTR Cl^- channels in cell-attached membrane patches in the presence of permeant oxidants and reductants. Our results demonstrate that activation of the Cl^- conductance mediated by CFTR has a step that is sensitive to the redox status of pyridine nucleotides.

MATERIALS AND METHODS

Cells—Mouse NIH 3T3 fibroblasts were cultured by standard techniques in Dulbecco's modified Eagle's medium H + 10% fetal bovine serum supplemented with penicillin and streptomycin. The origin and culture of the CFT1 epithelial cell line have been reported (21). The construction and production of the murine amphotropic retrovirus vectors LCFSN and LISN have been described previously (22). LCFSN contains the normal human CFTR cDNA under transcriptional control of the promoter elements in the retrovirus vector long terminal repeat sequence and a neo^r (neomycin resistance) gene under control of an internal SV40 promoter. LISN contains the cDNA for the α-subunit of the interleukin-2 receptor and a neo^r gene and was used to generate control cells. 3T3 fibroblasts and CFT1 cells were infected with LCFSN or LISN. Drug-resistant clones were selected after growth in G418. Infected cells retained CFTR-associated properties beyond passage 20. For the studies reported here, cells of passages 10–16 were subcultured onto 35-mm plastic dishes. Sf9 cells were grown in Spinner flasks in Grace's medium (23). Cells were subcultured onto 35-mm plastic dishes and exposed to a plaque pure baculovirus modified by replacement of the viral polyhedron gene with the human CFTR gene or with the β-galactosidase gene. Infected Sf9 cells were killed by viral infection within 48–72 h. High levels of CFTR protein were expressed by 36 h by immunoblot analysis. Insect cells were used for whole cell voltage clamp within 24–40 h of infection. T84 cells, a human colonic carcinoma cell line that expresses CFTR (24), were obtained from ATCC and maintained in Dulbecco's modified Eagle's medium with high glucose (4.5 g/liter) supplemented with 10% fetal bovine serum, penicillin, and streptomycin.

Immunoblot Analysis of CFTR Protein—CFTR protein was detected by the method of Sarkadi *et al.* (25) using purified polyclonal rabbit antibodies raised against synthetic human CFTR peptides as described previously. 3T3 fibroblasts and CFT1 cells were grown to confluence in plastic flasks, washed with phosphate-buffered saline, and harvested by trypsinization. Sf9 cells were collected and washed. Whole cell protein was extracted by suspension of cells in 6% (w/v) trichloroacetic acid and collection of the precipitate as a pellet (5,000 × *g*, 5 min). The pellet was dissolved in sodium dodecyl sulfate disaggregation buffer (50 mM Tris phosphate (pH 6.8), 2% (w/v) sodium dodecyl sulfate, 15% (w/v) glycerol, 2% (v/v) β-mercaptoethanol, 1 mM EDTA, and 0.02% (w/v) bromphenol blue). Electrophoresis of protein samples was carried out using 4–15% gradient acrylamide gels (Bio-Rad). Electroblotting of the proteins to polyvinylidene difluoride membranes (Bio-Rad) was carried out as described previously (25).

Patch Clamp Techniques—Cells were studied on the stage of an inverted microscope at 22 °C by the techniques of Hamill *et al.* (26). For most whole cell studies, pipettes (2–6 megohms) were filled with an intracellular buffer with the following composition, in mM/liter: Tris(hydroxymethyl)aminomethane gluconate, 100; Tris-Cl^-, 40; $MgCl_2$, 2; and TES, 5 (pH 7.2), and MgATP, 3. Ca^{2+} activity was buffered to approximately 40 nM (1.0 mM EGTA and 0.1 mM $CaCl_2$; calculated with Chelator Software, Th. Schoenmakers). Bath solutions for mammalian cells contained Tris-Cl or NaCl, 150; $MgCl_2$, 2; $CaCl_2$, 1; TES, 5; sucrose, 30; and D-glucose, 10. Voltage was clamped at −40 mV and stepped to 60 mV every 10 s for 0.4 s. Whole cell current voltage plots were obtained from the currents recorded in response to a series of voltage steps from zero, covering the range −80–140 mV in 20-mV increments. The effect of I^- on whole cell Cl^- currents was assessed after diluting the bath solution with 150 mM NaI extracellular buffer. For Sf9 cells the bath was NaCl, 132; $CaCl_2$, 5; $MgCl_2$, 4; TES, 10 (pH 6.7); and glucose, 10. Cell-attached recordings were carried out in 3T3 fibroblasts expressing CFTR. In this paradigm the Cl^- concentration in the pipette solution was either 155 NaCl or a combination of 40 mM Tris-Cl and 100 mM Tris gluconate.

Chemicals—Intracellular cAMP was raised by exposure to a combination of 25 μM forskolin (Sigma) and 0.5 mM CPT-cAMP (Sigma). The current sensitive to the stilbene DIDS was defined as the current inhibited by 0.5 mM DIDS (Aldrich). Adenosine triphosphate, guanine triphosphate, pyridine nucleotides, phenazine methosulfate (PMS), tert-butyl hydroxide (TBOH), and sodium metabisulfite (NaMBS) were purchased from Sigma.

Histone Phosphorylation—The effect of redox reagents on the activity of protein kinase A was investigated by a modification of the histone labeling procedure (27). Purified catalytic subunit of protein kinase A (Promega) was used to phosphorylate comparatively type IIA histone (Sigma) with [γ-^{32}P]ATP as the phosphate donor. The reaction products were trapped on phosphocellulose paper and γ emissions collected to quantitate the transfer of ^{32}P to histone. Control reaction buffer contained protein kinase A (150 nM/liter), 3 mM [γ-^{32}P]ATP, 1 mg/ml type IIA histone, 0.25 mg/ml bovine serum albumin, 10 mM $MgCl_2$, 50 mM TES (pH 7.2). Test buffers had the same composition with the addition of 1 mM/liter of one of the following: NAD^+, NADH, $NADP^+$, NADPH. In the absence of protein kinase A, transfer of ^{32}P to histone was not different from background for any reaction conditions.

Statistical Analyses—Drug-induced changes in whole cell current and differences between means were assessed for statistical significance by paired *t* tests (28).

RESULTS

Expression of CFTR protein in Sf9 (insect), NIH 3T3 (mouse fibroblast), and CFT1 (human cystic fibrosis airway epithelia) cells was verified by Western blot analysis (Fig. 1*A*). CFTR expressed in Sf9 cells infected with the baculovirus vector containing the human CFTR cDNA was detected as a 140-kDa band by Western blot analysis, consistent with previous reports that CFTR is not glycosylated in these cells (25). Protein extracted from 3T3 and CFT1 cells infected with the LCFSN vector contained a broad immunoreactive band in the 155–175-kDa region, a staining pattern expected of variably glycosylated CFTR protein (29), and similar to the staining of protein extracted from T84 cells. Whole cell Cl^- currents stimulated by a combination of forskolin (25 μM) and CPT-cAMP (0.5 mM) were measured as a functional assay of CFTR expression. Experiments that were carried out in Sf9 cells are illustrated in Fig. 1*B*. Forskolin and CPT-cAMP caused no significant change in basal currents in control Sf9 cells, including uninfected cells and cells infected with a recombinant baculovirus containing the cDNA for β-galactosidase. Forskolin and CPT-cAMP stimulated outward currents at 60 mV in cells that had been exposed to recombinant CFTR baculovirus. Stimulated currents in CFTR-expressing cells were insensitive to DIDS (14) but were inhibited by external I^- (Fig. 1*B*). The latter phenomenon was originally interpreted as an apparent greater selectivity for Cl^- over I^- by CFTR (14) but more recently as a block of anion permeation through CFTR Cl^- channels by concentrations of I^- less than about 150 mM (30, 31). Summary current-voltage relationships of basal and stimulated currents carried out in CFTR-expressing and sham-infected Sf9 cells, 3T3 fibroblasts, and CFT1 cells are shown in Fig. 1*C*. Cl^- was the major permeant anion in our solutions, and the cells were dialyzed with solution that contained no permeant cations. In each set of data the stimulated currents reversed near the reversal potential calculated from the Cl^- concentrations of pipette and bath solution and showed little voltage dependence. The data in Fig. 1 demonstrate expression of CFTR protein and Cl^- conductance function in three different expression systems.

Inhibition of oxidative metabolism, as employed in a previous study (1), is expected to decrease intracellular ATP but is also predicted to increase the ratio of reduced to oxidized pyridine nucleotides (9). We took advantage of whole cell dialysis to clamp intracellular ATP at 3 mM. Protocols to activate and characterize CFTR-mediated Cl^- currents (similar to that in Fig. 1*B*) were then carried out with either 1.2 mM NADPH or 0.3 mM $NADP^+$ in the pipette solution. When insect, fibroblast, or airway cells that expressed CFTR were dialyzed with NADPH, resting Cl^- currents tended to be less than control,

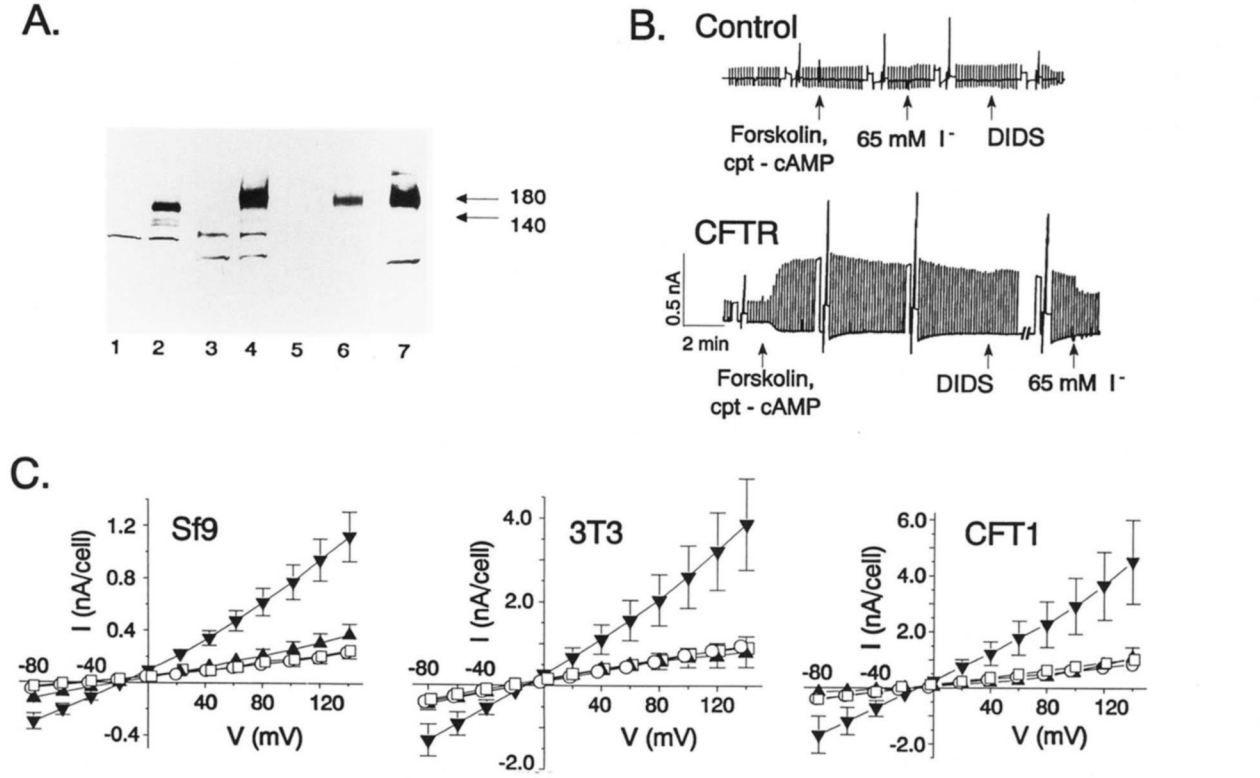

FIG. 1. **Expression of CFTR in three cell types detected by Western blot analysis and functional assay.** *Panel A*, immunoblot of whole cell lysates of CFTR-expressing and control cells. *Lane 1*, uninfected Sf9; *lane 2*, Sf9-CFTR; *lane 3*, 3T3-LISN; *lane 4*, 3T3-LCFSN; *lane 5*, CFT1-LISN; *lane 6*, CFT1-LCFSN; *lane 7*, T_{84}. Each lane was loaded with 30 μg of cell protein. *Panel B*, typical experiments in Sf9 cells to assess CFTR Cl^- conductance function. *Control* indicates uninfected. *CFTR* indicates ≈37-h exposure to baculovirus containing human CFTR cDNA. Clamp voltage was held at –40 mV and pulsed to 60 mV every 10 s for 0.4 s. The broad pulses were recorded at higher chart speed to allow better resolution. Current-voltage relationships were obtained after each high resolution pulse recording. Forskolin (25 μM), CPT-cAMP (0.5 mM), DIDS (0.5 mM), and I^- (65 mM) were present beginning at the times indicated by *arrows*. *Panel C*, current-voltage relationships before and during cAMP exposure. Control cells, basal (*circles*), and forskolin-exposed (*squares*) cells are compared with CFTR-expressing cells, basal (*right side-up triangles*) and forskolin exposed (*upside-down triangles*) cells.

and stimulation of current by forskolin and CPT-cAMP was decreased compared with CFTR-expressing cells studied with no pyridine nucleotide in the pipette solution (Fig. 2). In contrast, both the resting and stimulated currents in CFTR-expressing cells dialyzed with $NADP^+$ were greater than under control conditions. These effects of reduced and oxidized NADP on the cAMP-dependent Cl^- conductance associated with CFTR expression were found in Sf9 cells, in 3T3 fibroblasts, and in CFT1 airway epithelial cells. $NADP^+$/NADPH dialysis had no effect on currents recorded from uninfected cells (data not shown).

We verified that the elevated basal currents and large responses to cAMP in cells dialyzed with $NADP^+$ were mediated by CFTR. In the experiment illustrated in Fig. 3*A*, basal outward (Cl^-) current stabilized at 3 nA. Addition of forskolin and CPT-cAMP further increased current to nearly 5 nA. The current-voltage relationship for the large basal and stimulated currents were linear (Fig. 3, *B* and *C*) and reversed near E_{Cl} (Fig. 3*C*). Exchanging 120 mM bath solution NaCl with NaI sharply inhibited Cl^- current, to a value well below the non-stimulated resting current, and decreased whole cell conductance. The current-voltage relationship in the presence of I^- was depolarized (Fig. 3*C*), characteristic of the effect of external I^- on CFTR-mediated anion conductance. In a series of experiments, the inhibition of stimulated whole cell conductance by 75 mM I^- was larger in cells dialyzed with 0.3 mM $NADP^+$ than in cells dialyzed with control pipette solution (Fig. 3*D*), consistent with the larger conductance in the presence of oxidized NADP being mediated by CFTR.

To explore the mechanism of inhibition of CFTR-mediated Cl^- conductance by NADPH, we compared the effects of

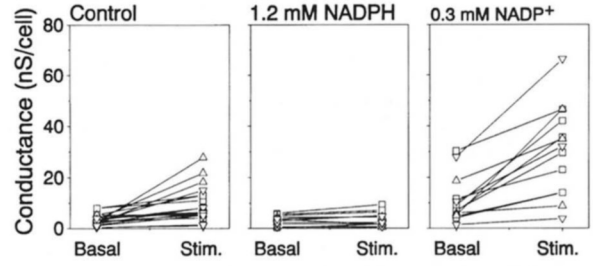

FIG. 2. **Effects of NADP on whole cell basal and cAMP-stimulated Cl^- conductance in CFTR-expressing cells.** *Left panel*, normal pipette solution with no pyridine nucleotide in the pipette solution. *Middle panel*, normal pipette solution with 1.2 mM NADPH in the pipette. *Right panel*, normal pipette solution with 0.3 mM $NADP^+$ in the pipette. CFTR-expressing cells: Sf9-CFTR (*upside-down triangles*), CFT1-LCFSN (*right side-up triangles*), and 3T3-LCFSN (*squares*). *nS*, nanosiemens.

NADPH dialysis on forskolin/CPT-cAMP-stimulated Cl^- conductance to the effects of NADH dialysis. As demonstrated above, CFTR-expressing cells dialyzed with NADPH typically responded to forskolin and CPT-cAMP with no changes in outward current (Fig. 4A) and whole cell conductance (Fig. 4*B*). In cells dialyzed with 1.2 mM NADH, forskolin and CPT-cAMP consistently induced increases in outward current (Fig. 4*A*) and conductance (Fig. 4*B*), but the forskolin/CPT-cAMP-induced conductance (3.0 ± 0.6 nanosiemens, $n = 7$) was significantly ($p < 0.03$) smaller than the response in control experiments (8.01 ± 0.18 nanosiemens, $n = 8$). We reasoned that if the inhibition of cAMP-stimulated Cl^- conductance was caused by the reduced status of the pyridine nucleotide, then a maneuver to shift the redox ratio to a more oxidized state should allow

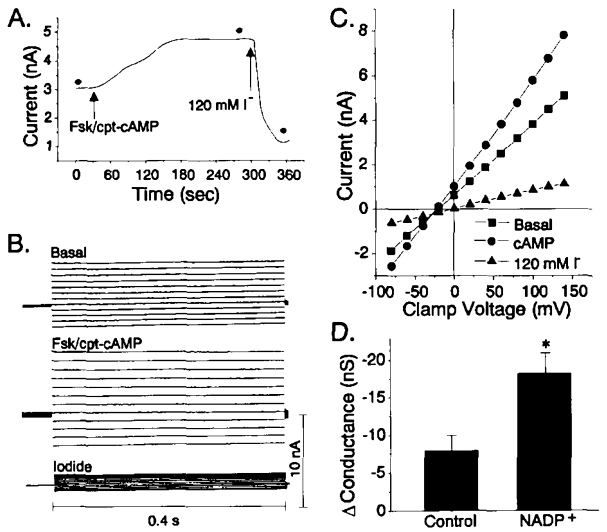

FIG. 3. **Elevated basal and cAMP-stimulated currents in 3T3 LCFSN cells dialyzed with 0.3 mM NADP⁺.** *Panel A*, peak outward Cl^- current in a cell dialyzed with $NADP^+$. The holding potential was −40 mV. Every 10 s, the clamp potential was stepped to 60 mV for 0.4 s. The outward current is recorded 0.1 s after the voltage is stepped to 60 mV. Forskolin (25 μM) and CPT-cAMP (0.5 mM) were added at the *first arrow* and maintained throughout the experiment. At 300 s the bath solution was changed to one in which 120 mM NaCl was replaced by 120 mM NaI. *Panel B*, families of currents measured in response to voltage stepped from a holding potential of 0 mV to a range of voltage from −80 to 140 mV in 20-mV increments. Each clamp voltage was maintained for 400 ms. These traces were obtained during the experiment shown in *panel A* at the times indicated by the *dots* (●) *Fsk*, forskolin. *Panel C*, plots of current-voltage data displayed in *panel B*. *Panel D*, the change in whole cell conductance induced by 75 mM I^- in cells dialyzed with pipette solution that contained no pyridine nucleotides (*Control*, $n = 9$) or 0.3 mM $NADP^+$ ($n = 8$). *Different from control by unpaired t analysis ($p < 0.005$). *nS*, nanosiemens.

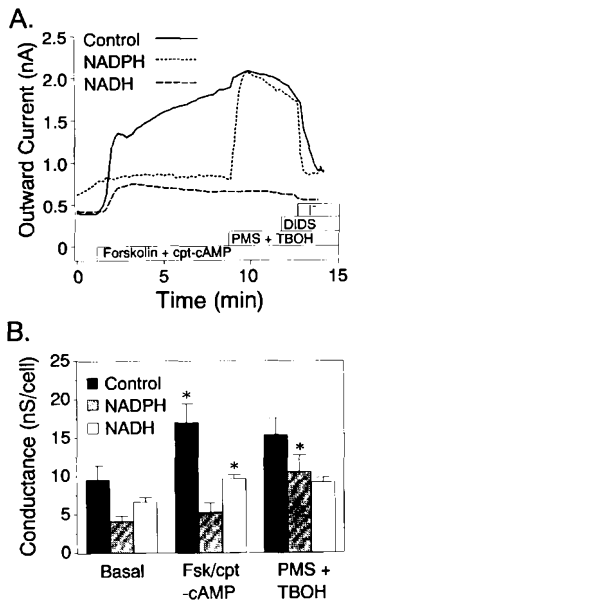

FIG. 4. **Inhibition of CFTR Cl^- conductance by reduced pyridine nucleotides.** *Panel A*, representative experiments in 3T3-LCFSN cells dialyzed with regular pipette solution (*Control*) or with pipette solution that contained 1.2 mM NADPH or 1.2 mM NADH. The holding voltage was −40 mV, and outward current at 60 mV was recorded every 10 s. Additions were made to the bath at the times indicated, with the following concentrations: forskolin, 25 μM; CPT-cAMP, 0.5 mM; TBOH, 2.5 mM; PMS, 2.5 mM; DIDS, 0.5 mM; I^-, 75 mM. *Panel B*, effect of reduced pyridine nucleotides on whole cell conductance of 3T3-LCFSN cells under basal conditions, during exposure to forskolin (*Fsk*) and CPT-cAMP and during exposure to PMS and TBOH. Pipette solutions as described in *panel A*. Control ($n = 9$), NADPH ($n = 7$), NADH ($n = 7$). *Different from preceding period by paired t analysis with Bonferroni adjustment for multiple comparisons ($p < 0.05$). *nS*, nanosiemens.

current to increase. To test this notion we added the cell-permeant electron carrier PMS to the bath (2.5 mM). TBOH was included (2.5 mM) to assure that PMS was fully oxidized. We expected oxidized PMS to enter the cell and oxidize a portion of cytosolic NADPH or NADH. Strikingly, the block of cAMP activation of current in CFTR-expressing cells that were dialyzed by 1.2 mM NADPH was overcome by this maneuver (Fig. 4, *A* and *B*). The newly stimulated conductance had identifying characteristics of cAMP-dependent CFTR-mediated conductance, including reversal of the current-voltage plot near the predicted reversal potential of a pure Cl^- current (−25 *versus* −33 mV, not shown), resistance to 0.5 mM DIDS, and inhibition by 75 mM I^- (Fig. 4*A*). In the same protocol, the inhibition of cAMP-dependent outward current (Fig. 4*A*) and whole cell conductance (Fig. 4*B*) by 1.2 mM NADH was not reversed by the PMS/TBOH oxidant cocktail. PMS and TBOH had no effect on whole cell currents of cells not expressing CFTR (not shown).

We extended the study of how pyridine nucleotides affect CFTR function by measuring the current and conductance in stimulated cells that were dialyzed with regular pipette solution or with 0.3 mM $NADP^+$ or NAD^+. We also tested whether a cell-permeant reducing agent (NaMBS) (32) would affect current stimulated in the presence of oxidized pyridine nucleotides in the pipette. The experiment in Fig. 5*A* is representative. Outward Cl^- current of a CFTR-expressing cell dialyzed with pipette solution that contained 0.3 mM NAD^+ was stimulated with forskolin and CPT-cAMP. NaMBS (3 mM) reversed this stimulation. The inhibition induced by NaMBS was not altered by the electron carrier PMS, which would be highly reduced in the presence of metabisulfite, but was overcome by introduction of the oxidant TBOH. The current manipulated by interactions between cytosolic pyridine nucleotides and permeant reductants and oxidants in this experiment was inhibited by 75 mM external I^-. Data from similar experiments comparing NaMBS inhibition of forskolin/CPT-cAMP-stimulated currents in cells dialyzed with normal pipette solution or pipette solution containing $NADP^+$ or NAD^+ are summarized as whole cell conductance in Fig. 5*B*. The larger whole cell conductance recorded with oxidized pyridine nucleotides in the pipette was more inhibited by the permeant reducing agent, suggesting that the oxidized state of the pyridine nucleotides was important for CFTR-mediated Cl^- conductance.

The single channel basis of CFTR-mediated Cl^- conductance has been reported to be a 4–8 picosiemens, slowly gating anion channel (15–18). We reasoned that modulation of CFTR-mediated whole cell conductance by permeant oxidants and reductants should be paralleled by effects on single CFTR Cl^- channels. In five of seven attempts in cell-attached membrane patches of 3T3 fibroblasts expressing CFTR, forskolin and CPT-cAMP induced the appearance of small, slowly gating channels, similar to what has been reported for CFTR Cl^- channels in other studies (Fig. 6*A*) (15–18). No channels were activated by forskolin and CPT-cAMP in fibroblasts not expressing CFTR ($n = 3$, not shown). The mean current-voltage relationships for cAMP-dependent channels from cell-attached recordings in stimulated cells revealed no marked voltage dependence and a single channel conductance of approximately 6 picosiemens in the range of $-V_{pipette}$ from 10 to 60 mV (Fig. 6*B*). The zero current voltage was 22 mV with 45 mM Cl^- in the pipette and 0 mV with 155 Cl^- in the pipette, indicating Cl^- selectivity (Fig. 6*B*). As reported previously, endogenous Cl^- channels were present in both infected (Fig. 6*C*, all traces) and uninfected cells

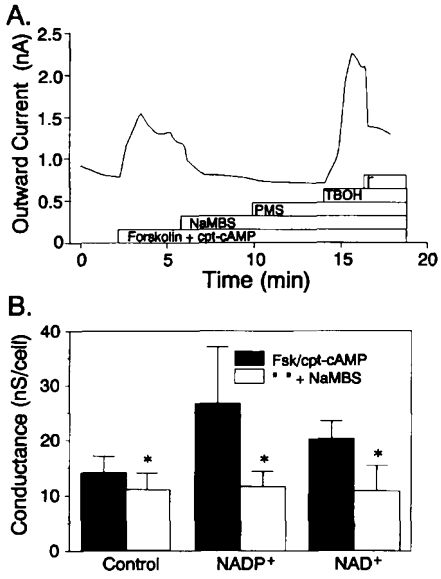

FIG. 5. **Modulation of cAMP-dependent Cl^- conductance in CFTR-expressing 3T3 fibroblasts by $NADP^+$ and NAD^+.** *Panel A*, outward current in a 3T3-LCFSN cell dialyzed with 0.3 mM NAD^+. Additions were made to the bath as indicated, at the following concentrations: forskolin, 25 μM; CPT-cAMP, 0.5 mM; TBOH, 2.5 mM; PMS, 2.5 mM; NaMBS, 3 mM. Bath solution was replaced a 50 mM NaI solution (final nominal concentrations 105 mM NaCl, 50 mM NaI). *Panel B*, whole cell conductance under cAMP-stimulated conditions in CFTR-expressing cells dialyzed with regular pipette solution (*Control* = no pyridine nucleotides, $n = 5$), with 0.3 mM $NADP^+$ ($n = 7$) or with 0.3 mM NAD^+ ($n = 5$). After steady-state stimulated conductance (*solid bars*) was recorded, NaMBS was added to the bath at a final concentration of 3 mM, and a new steady-state conductance was reached within 3–8 min (*open bars*). *Different from forskolin/CPT-cAMP value ($p < 0.05$). *nS*, nanosiemens.

(not shown and (23)), but had a larger conductance, more rapid kinetics, and did not respond to CPT-cAMP (Fig. 6*C*). Introduction of permeant oxidants (PMS/TBOH) into the bath promptly increased the activity of CFTR Cl^- channels but did not affect the activity of an endogenous Cl^- channel present in the same patch (Fig. 6*C*, *third* and *fourth traces* from *top*). The effect on CFTR Cl^- channels induced by PMS/TBOH was an increased open probability compared with forskolin and CPT-cAMP alone ($p < 0.05$) (Fig. 6*D*). The addition of NaMBS partially reversed the increase in CFTR Cl^- channel open probability seen with PMS/TBOH ($p < 0.05$) (Fig. 6*C*, *bottom trace*, and Fig. 6*D*). These single channel studies generally parallel the effects of redox agents on cAMP-dependent whole cell currents in CFTR-expressing cells and thus support the interpretation that intracellular redox potential modulates the cAMP-dependent Cl^- conductance mediated by CFTR.

We explored whether pyridine nucleotide redox status affected currents other than cAMP-dependent Cl^- current by measuring currents induced in fibroblasts by hypotonic swelling. A clone of CFTR-infected 3T3 cells which expressed small quantities of CFTR protein and no cAMP-dependent Cl^- conductance (45) was used to test the effect of NADPH on non-CFTR-mediated conductances in fibroblasts. The presence of 1.2 mM NADPH in the pipette solution did not affect the whole cell current stimulated by hypotonic (0.5 isotonic) shock (compare Fig. 7, *A* and *B*). MDR protein, an ATP-binding cassette protein with a structure analogous to CFTR, was reported to mediate hypotonically induced Cl^- conductance (5, 6). In 3T3 fibroblasts infected with a viral construct containing the cDNA for MDR protein (5, 33) we found that stimulation of whole cell currents by hypotonic shock was not affected by NADPH in the

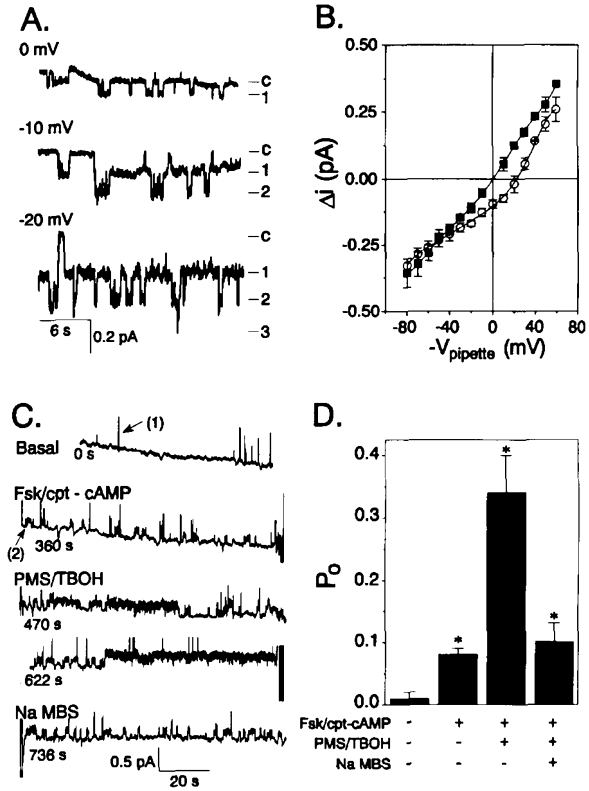

FIG. 6. **Redox-sensitive activity of cAMP-dependent CFTR Cl^- channels in 3T3 fibroblasts.** *Panel A*, current recorded in a cell-attached membrane patch during exposure to forskolin and CPT-cAMP. The pipette contained 45 mM Cl^- and poorly permeant cations (see "Materials and Methods"). The potentials above each trace represent the opposite of pipette potential, and anion channels open with downward deflections. To the *right* of each trace, *c* represents the closed state; *numbers* designate the levels of current jumps. *Panel B*, current voltage relationships of anion channels activated by forskolin and CPT-cAMP in the cell- attached mode. Current jumps (Δi) are plotted against the opposite of pipette voltage ($-V_{pipette}$). The pipette contained 155 mM Cl^- (*closed squares*) or 45 mM Cl^- (*open circles*). Positive current represents Cl^- entering the cell. Each *symbol* and *bars* represent the mean ± S.E. of four to seven separate experiments. Lines were fit by polynomial regression to the mean data. *Panel C*, recording from a cell-attached membrane patch of a 3T3 fibroblast-expressing CFTR. After gigaohm seal formation, the pipette current was monitored at 30 mV (pipette potential). The pipette contained 45 mM Cl^- and no permeant cations, and upward current jumps represent Cl^- entering the pipette. The experimental condition is printed at the *top left* of each trace, and the running time in the experiment is printed beneath the beginning of each trace. In the trace labeled *Basal*, *1* denotes a fast, upward opening anion channel, whose activity is unaffected by subsequent additions to the bath solution. The trace labeled *Fsk/CPT-cAMP* shows the last 100 s of exposure to forskolin and CPT-cAMP alone. *(2)* denotes a small, slowly gating channel that appeared with forskolin/CPT-cAMP exposure. PMS/TBOH was added at 460 s and caused the immediate appearance of two small anion channels that could each open for many seconds. At 725 s NaMBS was added to the bath and decreased the open probability of the small slow anion channels. *Panel D*, open probability (P_o) during unstimulated cell-attached recording and then in the presence of forskolin (*Fsk*) and CPT-cAMP, and with PMS/TBOH or with NaMBS. *Bars* represent the mean ± S.E. of P_o calculated from five experiments carried out with the protocol illustrated in *panel C*. P_o was calculated by a 50% threshold method, assuming that the maximum number of channels observed was present throughout with an equal and independent probability of opening. Each entire experiment was analyzed for P_o, a total of 1,075 s for basal, 1,415 s for forskolin and CPT-cAMP, 1,155 s for PMS/TBOH, and 835 s for NaMBS. *Different from preceding period ($p < 0.05$, paired t analysis with Bonferroni adjustment for three comparisons).

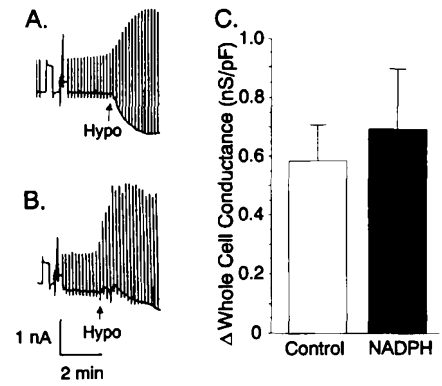

FIG. 7. **Effects of NADPH on swelling-induced whole cell currents.** *Panels A* and *B*, representative whole cell current traces from CFTR-expressing fibroblasts dialyzed with a K^+-rich buffer (in mM/liter: KCl, 110; $MgCl_2$, 2; and TES, 5 (pH 7.2), and MgATP, 3. Ca^{2+} activity was buffered to ≈40 nM (1.0 mM EGTA and 0.1 mM $CaCl_2$)). After steady state the bath was diluted by 50% with a solution of 2 mM $MgCl_2$, 1 mM $CaCl_2$, and 5 mM TES to induce a swelling current. *Panel A*, the control had no pyridine nucleotides in the K^+-rich pipette solution. *Panel B*, 1.2 mM NADPH in the K^+-rich pipette solution. *Panel C*, increment in whole cell conductance induced by hypotonicity (0.5 isotonic) was measured in fibroblasts expressing the MDR protein, either in the absence (control) or presence of 1.2 mM NADPH in the K^+-rich buffer pipette solution described in *panel A* (n = 5–6 in each group). *nS*, nanosiemens; *pF*, picofarad.

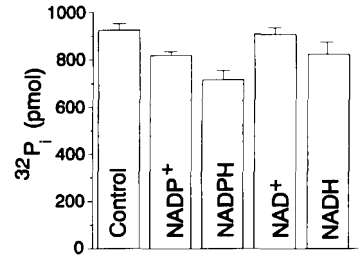

FIG. 8. **Protein kinase A activity under oxidizing and reducing conditions.** Protein kinase A activity was measured as the ability to phosphorylate histone IIA *in vitro* in the presence of a 1 mM concentration of each of the following oxidizing and reducing agents: no addition, $NADP^+$, NADPH, NAD^+, and NADH.

pipette (Fig. 7*B*). Thus, modulation of cAMP-dependent Cl^- current by NADP redox status is a characteristic of CFTR-mediated Cl^- conductance not shared by other conductances in fibroblasts.

Under the conditions of our experiments, *i.e.* high levels of CFTR expression, constant 3 mM ATP, and permeant cAMP, the only protein elements known to be required for cAMP-dependent activation of CFTR-mediated whole cell Cl^- currents are CFTR and endogenous protein kinase A. To determine if redox potential could affect the function of protein kinase A, we examined the protein kinase A-mediated incorporation of ^{32}P into histone in reaction mixtures that contained oxidized or reduced nucleotides. As summarized in Fig. 8, neither reduced nor oxidized pyridine nucleotides had significant effects on protein kinase A function.

DISCUSSION

In sweat ductal and airway epithelia, apical membrane Cl^- conductance has been reported to diminish under conditions of metabolic inhibition. Apical membrane Cl^- conductance is traditionally modeled as a process with the characteristics of passive ion diffusion, so the apparent metabolic dependence of Cl^- conductance was unpredicted. CFTR has been identified as the epithelial cAMP-dependent Cl^- conductance. CFTR has consensus nucleotide binding sites which have been proposed to bind or hydrolyze ATP, and ATP concentration at the cytosolic membrane surface has been implicated in the regulation of CFTR Cl^- conductance in sweat ductal epithelium and gating of CFTR channels in excised membrane patches (7, 8). Intracellular ATP concentration has been proposed to couple apical membrane Cl^- conductance to metabolic state. In the present study, however, we clamped intracellular ATP at a physiologic concentration and found that variation of pyridine nucleotide redox potential affected CFTR Cl^- conductance. When three diverse cell types that expressed CFTR were dialyzed with reduced pyridine nucleotides, cAMP-dependent Cl^- current was diminished. Conversely, during dialysis of CFTR-expressing cells with oxidized pyridine nucleotides, basal currents were larger, and the responses of CFTR-mediated Cl^- currents to cAMP were enhanced. Because ATP concentration is not expected to have changed during these experiments, the results show that redox potential chemically clamped by NAD(P)H and $NAD(P)^+$ modulates CFTR Cl^- conductance.

Several observations confirmed that the Cl^- currents affected by pyridine nucleotides in CFTR-expressing cells were indeed mediated by CFTR. First, the currents of uninfected cells of epithelial, nonepithelial, and insect origin, which demonstrated no cAMP-dependent Cl^- current, were unaffected by dialysis with oxidized or reduced nucleotides or by exposure to permeant oxidants and reductants. Second, the Cl^- currents activated by cAMP in CFTR-expressing Sf9, CFT1, and 3T3 cells exposed to intracellular oxidized pyridine nucleotides were DIDS-insensitive and were inhibited by external I^-, two important characteristics of cAMP-dependent Cl^- currents mediated by CFTR. Most definitively, we recorded single CFTR Cl^- channels in cell-attached membrane patches of 3T3 cells expressing CFTR and found that the activity of these channels was modulated by permeant oxidants and reductants in a way that was consistent with the modulation of whole cell Cl^- conductance.

The mechanism by which the redox status of intracellular pyridine nucleotides affects CFTR Cl^- conductance is unknown. Under the conditions of our experiments, CFTR and protein kinase A are the only proteins with well established roles in the activation of cAMP-dependent Cl^- conductance (3). Required soluble reactants, *i.e.* ATP and cAMP, were provided exogenously, and we determined that redox potential clamped by pyridine nucleotides had no effect on the ability of protein kinase A to phosphorylate histone. Other regulatory proteins known to interact with CFTR, such as protein kinase C (35), cGMP-dependent kinase (36), and protein phosphatases (16), do not require pyridine nucleotides as cofactors. Thus, modulation of cAMP-dependent Cl^- currents by cytosolic NAD(P)/NAD(P)H could be explained by reversible regulation of the CFTR protein itself. Perhaps more plausible, however, is the possibility that CFTR may interact with proteins not yet identified but nonetheless important for cAMP-activated Cl^- conductance, such as cytoskeletal elements. Either the function of such putative proteins or their possible interactions with CFTR could be influenced by pyridine nucleotide redox potential.

The differential effects of NAD and NADP on CFTR Cl^- conductance function may allow some speculation as to the nature of the mechanism(s) by which pyridine nucleotides affect CFTR. Although NADH, like NADPH, inhibited activation of CFTR Cl^- conductance by cAMP, inhibition by NADH was not as complete and was not reversed by permeant oxidants. Moreover, whereas cells dialyzed with NAD^+ very consistently responded to forskolin and CPT-cAMP with characteristic

CFTR Cl^- conductance, the largest responses occurred in cells dialyzed with $NADP^+$. It is not uncommon for proteins to exhibit different relative affinities for reduced and oxidized forms of NADP and NAD. For example, the order of affinities for pyridine nucleotide binding to catalase is NADPH > NADH > $NADP^+$ > NAD^+ (44). Thus, tight binding of NADPH to CFTR, or a CFTR-associated protein, can be speculated to favor a CFTR conformation that is not activated by cAMP-dependent phosphorylation, whereas NADH may have a weaker binding affinity for the same site. Dialysis of CFTR-expressing cells with high concentrations of reduced nucleotides would then account for the inhibition of CFTR which we observed. Under the oxidized conditions imposed by dialysis with $NADP^+$, or by exposure of NADPH dialyzed cells to permeant oxidants, NADPH bound to CFTR would be displaced by or converted to $NADP^+$, relieving NADPH-mediated inhibition of Cl^- conductance. NADH dialysis may mediate inhibition of CFTR which cannot be reversed by exposure to permeant oxidants because this maneuver would convert a portion of NADH to NAD^+, speculated to be the least avidly bound nucleotide and perhaps unable to compete with NADH for binding.

Alternatively, the greater effectiveness of the NADPH/$NADP^+$ couple may indicate that redox modulation of CFTR Cl^- conductance is mediated through the activity of enzymes that prefer NADPH over NADH. This specificity is a characteristic of enzymes, such as glutathione *S*-transferase, glutathione reductase, and protein disulfide isomerase, which utilize the typically highly reduced status of NADPH to maintain protein cysteines and free intracellular glutathione in a reduced state (10). Although CFTR has 17 cysteines, 12 of which are highly conserved among CFTRs from different species (human, rat, mouse, dogfish) (37–39), biochemical analyses of CFTR have not identified high molecular weight species that could be explained by intermolecular disulfide bond formation between CFTR molecules. Nonetheless, functional data routinely show that CFTR Cl^- channels appear in clusters (17) or exhibit cooperative gating patterns referred to as "wavelike" behavior (40, 41). Such observations strongly suggest that CFTR associates with itself and/or with cytoskeletal or other components in functioning as a Cl^- channel. Similar functional interactions of other ion channel proteins have been shown to be sensitive to redox potential, even when not due to formation of disulfide bonds (42).

The concentration of free pyridine nucleotides to which endogenous CFTR is normally exposed in intact, secretory epithelia is not well established. In a variety of rat tissues the total concentration of NADPH + $NADP^+$ is in a range of 200 μM, and the ratio NADPH/$NADP^+$ is more reduced than oxidized, whereas the tissue concentration of NADH + NAD^+ is approximately 500 μM, and NADH/NAD^+ is more oxidized than reduced (43). Values for NADP within this range were found in red blood cells (44) and in cultured airway epithelial cells.[2] The actual concentrations of reduced and oxidized pyridine nucleotides free in the cytosol are lower still but are difficult to predict because of tight protein binding and uneven distribution among cellular compartments (34). We selected concentrations of NAD(P)H (1.2 mM) and $NAD(P)^+$ (0.3 mM) which exceed likely physiologic concentrations to make a clear comparison between the effects of reduced and oxidized pyridine nucleotides on CFTR Cl^- conductance function. The metabolic rate and the ratio of ATP to ADP within cells are related to pyridine nucleotide redox status, such that a low ATP/ADP ratio caused by inhibition of oxidative metabolism is coincident with more reduced ratios of cytosolic free pyridine nucleotides (9). Conversely, more oxidized ratios of cytosolic free pyridine nucleotides arise from a high metabolic rate and high ATP/ADP ratio. The observation that CFTR-mediated, cAMP-dependent Cl^- conductance was modulated by NAD(P) redox status suggests that the reduced cytosolic redox potential in airway epithelia exposed to anoxia or NaCN might contribute to the inhibition of cAMP-dependent Cl^- conductance (1).

Metabolic regulation of CFTR-mediated Cl^- conductance has been proposed as an important mechanism by which active fluid secretion is coupled to the metabolic status of epithelial tissues. Quinton and Reddy (8) found recently that CFTR-mediated Cl^- conductance is regulated by intracellular ATP concentration. Our results suggest that variations in NAD(P) redox status expected to occur with different metabolic states could contribute to metabolic regulation of CFTR Cl^- conductance. Understanding the mechanism(s) by which intracellular pyridine nucleotides regulate CFTR-mediated cAMP-dependent Cl^- conductance could provide new insights into the functions of CFTR and new ideas for pharmacological therapeutic approaches to the treatment of cystic fibrosis or other diseases involving CFTR.

[2] H. N. Kirkman, personal communication.

REFERENCES

1. Stutts, M. J., Gatzy, J. T., and Boucher, R. C. (1988) *J. Appl. Physiol.* **64,** 253–258
2. Flockhart, D. A., Freist, W., Hoppe, J., Lincoln, T. M., and Corbin, J. D. (1984) *Eur. J. Biochem.* **140,** 289–295
3. Collins, F. S. (1992) *Science* **256,** 774–779
4. Higgins, C. F., Hiles, I. D., Whalley, K., and Jamieson, D. J. (1985) *EMBO J.* **4,** 1033–1040
5. Hyde, S. C., Emsley, P., Hartshorn, M. J., Mimmack, M. M., Gileadi, U., Pearce, S. R., Gallagher, M. P., Gill, D. R., Hubbard, R. E., and Higgins, C. F. (1990) *Nature* **346,** 362–365
6. Gill, D. R., Hyde, S. C., Higgins, C. F., Valverde, M. A., Mintenig, G. M., and Sepulveda, F. V. (1992) *Cell* **71,** 23–32
7. Anderson, M. P., Berger, H. A., Rich, D. P., Gregory, R. J., Smith, A. E., and Welsh, M. J. (1991) *Cell* **67,** 775–784
8. Quinton, P. M., and Reddy, M. M. (1992) *Nature* **360,** 79–81
9. Hedeskov, C. J., Capito, K., and Thams, P. (1987) *Biochem. J.* **241,** 161–167
10. Tietze, F. (1970) *Arch. Biochem. Biophys.* **138,** 177–188
11. Ran, S., and Benos, D. J. (1992) *J. Biol. Chem.* **267,** 3618–3625
12. Fuhrmann, G. F., Schwarz, W., Kersten, R., and Sdun, H. (1984) *Biochim. Biophys. Acta* **820,** 223–234
13. Ruppersberg, J. P., Stocker, M., Pongs, O., Heinemann, S. H., Frank, R., and Koenen, M. (1991) *Nature* **352,** 711–714
14. Haws, C., Krouse, M. E., Xia, Y., Gruenert, D. C., and Wine, J. (1992) *Am. J. Physiol.* **263,** L692–L707
15. Anderson, M. P., and Welsh, M. J. (1991) *Proc. Natl. Acad. Sci. U. S. A.* **88,** 6003–6007
16. Tabcharani, J. A., Chang, X. B., Riordan, J. R., and Hanrahan, J. W. (1991) *Nature* **352,** 628–631
17. Rommens, J. M., Dho, S., Bear, C. E., Kartner, N., Kennedy, D., Riordan, J. R., Tsui, L. C., and Foskett, J. K. (1991) *Proc. Natl. Acad. Sci. U. S. A.* **88,** 7500–7504
18. Berger, H. A., Anderson, M. P., Gregory, R. J., Thompson, S., Howard, P. W., Maurer, R. A., Mulligan, R., Smith, A. E., and Welsh, M. J. (1991) *J. Clin. Invest.* **88,** 1422–1431
19. Tabcharani, J. A., Low, W., Elie, D., and Hanrahan, J. W. (1990) *FEBS Lett.* **270,** 157–164
20. Gray, M. A., Pollard, C. E., Harris, A., Coleman, L., Greenwell, J. R., and Argent, B. E. (1990) *Am. J. Physiol.* **259,** C752–C761
21. Yankaskas, J. R., Haizlip, J. E., Conrad, M., Koval, D., Lazarowski, E., Paradiso, A. M., Schlegel, R., Sarkadi, B., and Boucher, R. C. (1993) *Am. J. Physiol.* **264,** C1219–C1230
22. Olsen, J. C., Johnson, L. G., Stutts, M. J., Sarkadi, B., Yankaskas, J. R., Swanstrom, R., and Boucher, R. C. (1992) *Hum. Gene Ther.* **3,** 253–266
23. Gabriel, S. E., Price, E. M., Boucher, R. C., and Stutts, M. J. (1992) *Am. J. Physiol.* **263,** C708–C713
24. Cohn, J. A., Nairn, A. C., Marino, C. R., Melhus, O., and Kole, J. (1992) *Proc. Natl. Acad. Sci. U. S. A.* **89,** 2340–2344
25. Sarkadi, B., Bauzon, D. D., Huckle, W., Earp, H. S., Berry, A., Suchindran, H., Price, E., Olsen, J., Boucher, R. C., and Scarborough, G. A. (1992) *J. Biol. Chem.* **267,** 2087–2095
26. Hamill, O. P., Marty, A., Neher, E., Sakmann, B., and Sigworth, F. J. (1981) *Pflügers Arch.* **391,** 85–100
27. Forsyth, G. W., and Gabriel, S. E. (1989) *J. Membr. Biol.* **107,** 137–144
28. Shott, S. (1990) *Statistics for Health Professionals,* pp. 342–346, Saunders, Philadelphia
29. Cheng, S. H., Rich, D. P., Marshall, J., Gregory, R. J., Welsh, M. J., and Smith, A. E. (1991) *Cell* **66,** 1027–1036
30. Tabcharani, J. A., Chang, X.-B., Riordan, J. R., and Hanrahan, J. W. (1992) *Biophys. J.* **62,** 1–4
31. Bell, C. L., and Quinton, P. M. (1992) *Am. J. Physiol.* **262,** C555–C562

32. Parker, J. C. (1969) *J. Clin. Invest.* **48,** 117–125
33. Valverde, M. A., Diaz, M., Sepulveda, F. V., Gill, D. R., Hyde, S. C., and Higgins, C. F. (1992) *Nature* **355,** 830–833
34. Krebs, H. A. (1967) *Adv. Enzyme Regul.* **5,** 405–434
35. de Jonge, H. R., van den Berghe, N., Tilly, B. C., Kansen, M., and Bijman, J. (1989) *Biochem. Soc. Trans.* **17,** 816–818
36. Hwang, T. C., Lu, L., Zeitlin, P. L., Gruenert, D. C., Huganir, R., and Guggino, W. B. (1989) *Science* **244,** 1351–1353
37. Tata, F., Stanier, P., Wicking, C., Halford, S., Kruyer, H., Lench, N. J., Scambler, P. J., Hansen, C., Braman, J. C., Williamson, R., and Wainwright, B. J. (1991) *Genomics* **10,** 301–307
38. Diamond, G., Scanlin, T. F., Zasloff, M. A., and Bevins, C. L. (1991) *J. Biol. Chem.* **266,** 22761–22769
39. Marshall, J., Martin, K. A., Picciotto, M., Hockfield, S., Nairn, A. C., and Kaczmarek, L. K. (1991) *J. Biol. Chem.* **266,** 22749–22754
40. Bear, C. E., Duguay, F., Naismith, A. L., Kartner, N., Hanrahan, J. W., and Riordan, J. R. (1991) *J. Biol. Chem.* **266,** 19142–19145
41. Larsen, E. H., Fullton, J., Stutts, M. J., Boucher, R. C., and Price, E. (1992) *Pediatr. Pulmonol.* **Suppl. 8,** 267 (abstr.)
42. Schindler, H., Spillecke, F., and Neumann, E. (1984) *Proc. Natl. Acad. Sci. U. S. A.* **81,** 6222–6226
43. Glock, G. E., and McLean, P. (1955) *Biochem J.* **61,** 388–390
44. Gaetani, G. F., Galiano, S., Canepa, L. Ferraris, A. M., and Kirkman, H. N. (1989) *Blood* **73,** 334–339
45. Stutts, M. J., Gabriel, S. E., Olsen, J. C., Gatzy, J. T., O'Connell, T. L., Price, E. M., and Boucher, R. C. (1993) *J. Biol. Chem.* **268,** 20653–20658